CrossMark

Investigation of Metal Magnetic Memory Signals of Welding Cracks

Kunshan Xu[1] · Xingqi Qiu[2] · Xiaoshuai Tian[2]

Abstract Metal magnetic memory (MMM) testing is an advanced and nondestructive testing method based on magneto-mechanical effects. This technique can be used to assess defects based on MMM signals (MMMS). However, a thorough understanding of the impact that crack depth, working load, and heat treatment have on residual magnetic field variations (which can in turn affect defect assessment) has not yet been established in the literature. This report presents MMMS testing results of buried welding cracks under different applied loads, as well as before and after heat treatment, in order to analyse the impact of such factors on MMMS data. The results show that the MMMS is significantly affected by the depth at which a given crack is buried in a material, any load applied to the specimen, and the type of heat treatment employed. Therefore, the above factors should be considered when evaluating defects to avoid the inappropriate assessment of such defects.

Keywords Metal magnetic memory · Defect evaluation · Welding crack · Crack depth · Applied load · Heat treatment

1 Introduction

As a novel magnetic testing method [1–4], metal magnetic memory (MMM) techniques have proven to be effective in characterizing stress concentration and defects in ferromag-

netic materials. The physical mechanism of MMM has been examined in detail elsewhere [5]; in brief, under the effects of earth field and mechanical loads, self-magnetic-flux-leakage (SMFL) signals are generated in stress-concentration zones where the tangential SMFL component $H_P(x)$ reaches the maximum and the normal component $H_P(y)$ changes polarity and has a zero value. This magnetic state is retained even if the load is removed. From the viewpoint of micro-structures, this behaviour is attributed to the irreversible orientation of magnetic domains in stress-concentration zones. In recent years, MMM has received extensive attention in engineering fields due to its ease of use, short analysis time, and simple setup [6–10]. The correlation of $H_P(y)$ and its gradient K with loading cycles and applied magnetic field intensity H has been examined previously [11,12], and the universality of this algorithm for the evaluation of first-order residual stress using gradients of the residual magnetic field components has also been studied [13]. Roskosz [14] conducted a comparative study of magnetic memory signal and stress distribution in welding cracks. Various applications of diagnosing pressure vessels and others have also been reported [15–18]. MMM has been used to monitor damage development in steel tubes and welded joints [19], and the distribution of self-magnetic flux leakage (SMFL) based on the theory of magnetic charges has also been investigated [20,21].

However, a thorough understanding of the impacts of buried cracks (typical defects in welded joints), working load, and heat treatment on the residual magnetic field variations that affect defect assessment has not been clearly established. First, the impact of buried cracks on leakage magnetic field must be studied. Second, because most metal components are subject to a certain working load, the impact of working load on MMM signals (MMMS) is also a key point to be studied. Third, some metal components in welding processes are usually subject to heat treatment, and the stress distribu-

✉ Kunshan Xu
17911162@qq.com

[1] Yantai University, No.30, Qingquan Road, Yantai, Shandong, China

[2] China University of Petroleum (East China), Shandong, China
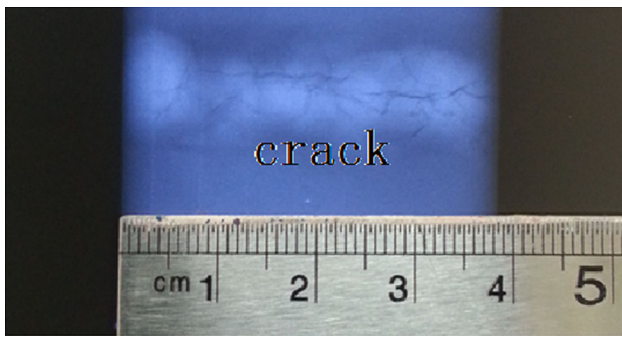
Fig. 1 Radiogram of crack H1

Fig. 3 Radiogram of crack H2

tion of the metal components after heat treatment is likely to change, affecting the magnetic field distribution of the metal components. Therefore, the impact of heat treatment on the magnetic memory signals of welding cracks is also worth examining. In view of these shortcomings, this paper studies the impacts of crack depth, applied load, and heat treatment on magnetic memory signals. The results obtained herein are valuable for MMM applications in assessing crack defects.

2 MMM Testing of Welded Joints

Ten specimens were fabricated to investigate the characteristics of MMMS of crack. The signal in the crack position followed all obvious change laws. Two typical specimens of the same size were selected to exhibit the change laws. The first specimen contained multiple cracks (H1), while the second specimen contained only one crack (H2). The dimensions of both H1 and H2 are 10 mm × 40 mm × 500 mm.

2.1 Welding Crack Analysis

X-ray testing was used to indicate the cracks in specimen H1, as shown in Fig. 1.

As can be seen from Fig. 1, H1 contains multiple irregular cracks. Ultrasonic detection results provide the buried depths
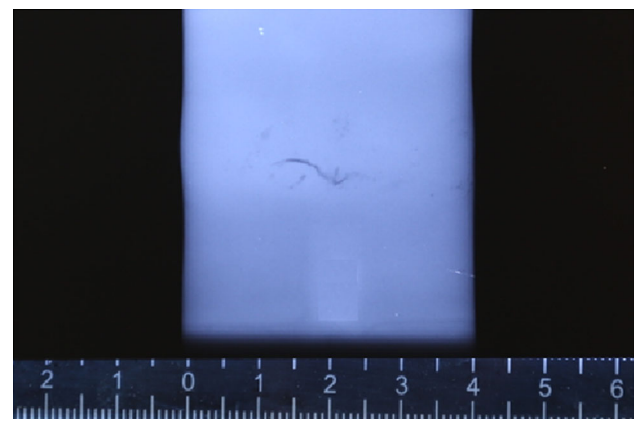
of the cracks, and the location where the highest reflected wave appeared (Fig. 2).

The distance between the centre of the probe, where the peak value of the ultrasonic wave appeared, and the edge of the specimen is 24.5 mm, whereas the reflected wave from ultrasonic testing decreased to 40% of the highest reflection wave in two contrasting directions (distances of 21 and 31 mm, respectively). The ultrasonic testing results show that the cracks are located at depths of 6.1, 7.6, and 6.8 mm. Therefore, the cracks are not parallel to the surface of the sample, and the distance from the cracks to the upper surface is greater than that to the lower surface. This also implies that the depths of the cracks are greater when tested from the upper surface compared to testing from the lower surface.

X-ray detection results of specimen H2 are shown in Fig. 3, which indicate that H2 contains only one crack.

2.2 Testing Procedure

Tests were conducted by scanning the surface of a welded joint perpendicular to the axis of the weld seam; a testing device with four sensors was used to scan the entire weld
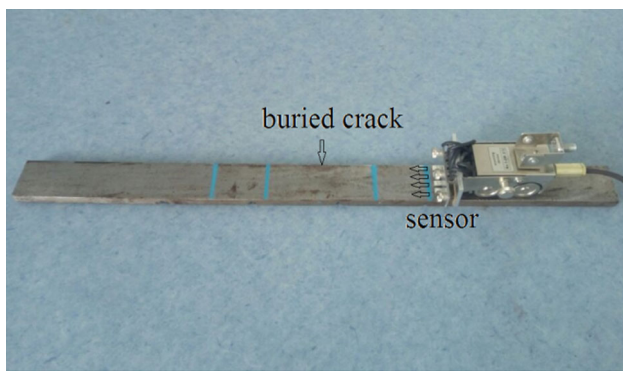
Fig. 2 Ultrasonic testing results of H1
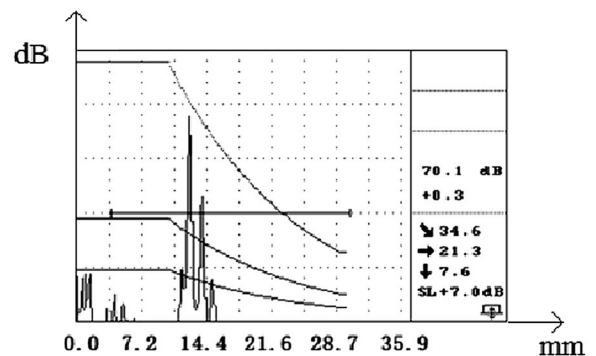
Fig. 4 Measurement process

seam. The distribution of the sensors along the length of the specimen with crack is shown in Fig. 4.

The MMM testing results of the upper and lower surfaces of H1 are presented to study the influence of the depth of the buried crack on MMMS. H1 was then tested under different applied loads to study the impact of load strength on MMMS. Stress-relieving heat treatment was conducted on H2, and compared to the results of H2 before heat treatment.

3 Results and Discussion

In this study, all odd testing result channels are tangential components, and all even channels are normal components.

3.1 Impact of Crack Depth on MMM Signal

The testing results of the upper surface of specimen H1 are listed in Fig. 5a–d, and those of the lower surface are listed in Fig. 6a–d.

3.1.1 Magnetic Field Intensity Tests

As can be seen in Fig. 5a, b, the tangential components of the magnetic field intensity reached their maximum values at the position indicated by 50 mm on the horizontal axis, and the normal components passed through zero. Moreover, the same results were obtained from the lower surface of the specimen (Fig. 6a, b). Therefore, the magnetic field intensity curve could accurately locate buried cracks. In addition, the peak value of the magnetic field intensity of the lower surface is higher than that of the upper surface due to the crack depth.

3.1.2 Magnetic Field Intensity Gradient Tests

As seen in Fig. 5c, the peak value of the tangential components tested from the upper surface of H1 is 12 (A/m)/mm, while the peak value tested from its lower surface is 30 (A/m)/mm (Fig. 6c). Similarly, the peak value of the normal components tested from the upper surface is 35 (A/m)/mm, while from the lower surface this value was 80 (A/m)/mm (Figs. 5d, 6d). For further comparison, the surface magnetic field measurement values of H1 are shown in Table 1.
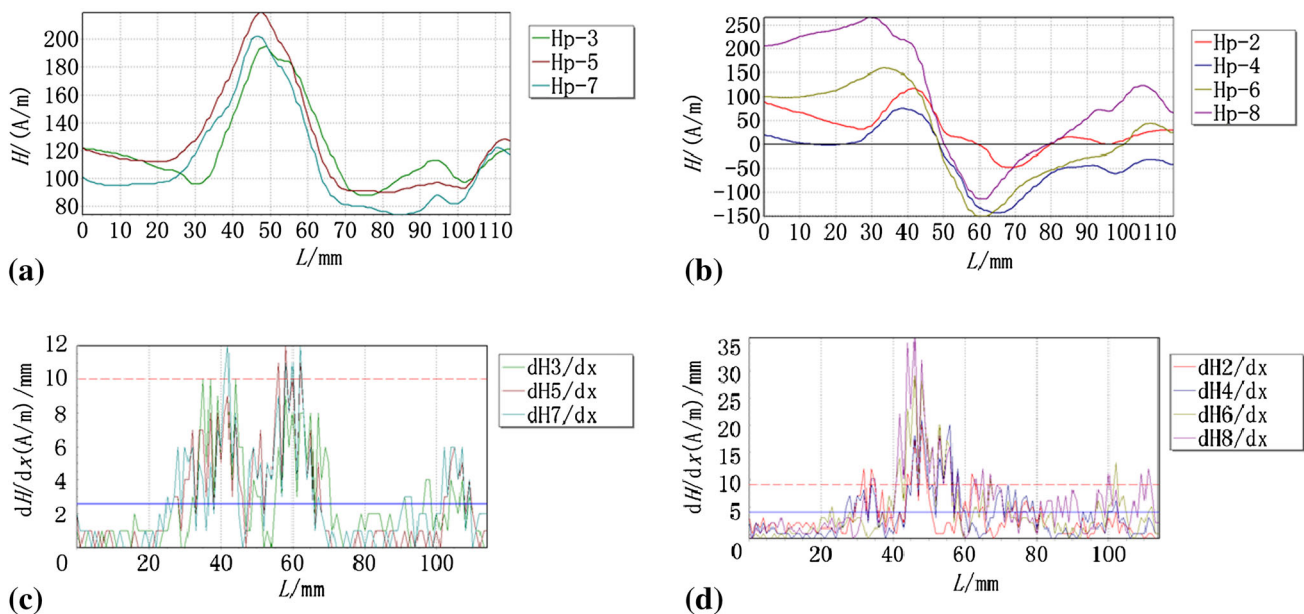

(a)

(b)

(c)

(d)

Fig. 5 Testing results of the upper surface of specimen H1. **a** Tangential components. **b** Normal components. **c** Gradient of tangential components. **d** Gradient of normal components
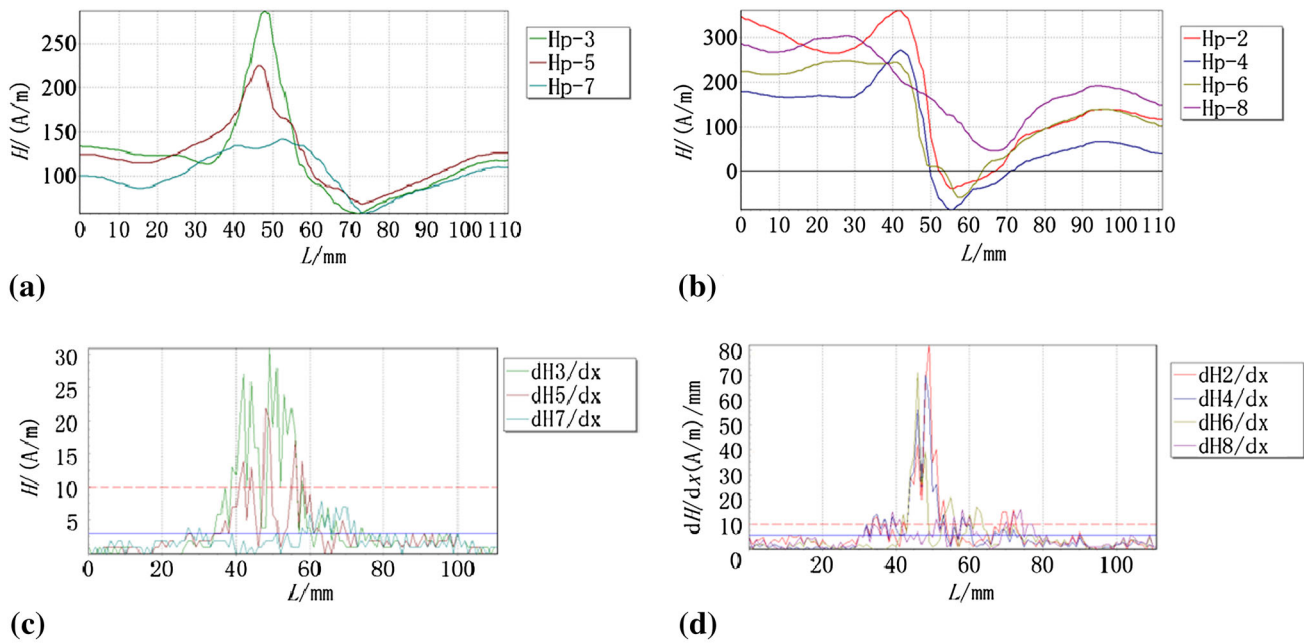
(a)

(b)

(c)

(d)

Fig. 6 Testing results of the lower surface of specimen H1. **a** Tangential components. **b** Normal components. **c** Gradient of tangential components. **d** Gradient of normal components

Table 1 Magnetic field parameters of buried welding cracks

Testing position	Crack depth (mm)	$\mid H_{P(x)\,max} - H_{P(x)\,max} \mid$ (A/m)	$\mid H_{P(y)\,max} - H_{P(y)\,max} \mid$ (A/m)	$dH_{P(x)}/dx$ (A/m)/mm	$dH_{P(y)}/dx$ (A/m)/mm
Upper surface	6.1, 7.6, 6.8	$\mid 218 - 75 \mid = 143$	$\mid 260 - (-150) \mid = 410$	12	35
Lower surface	3.9, 2.4, 3.2	$\mid 286 - 60 \mid = 226$	$\mid 360 - (-80) \mid = 440$	30	80

According to Table 1, the parameters $dH_p(x)/dx$ and $dH_p(y)/dx$ tested from the lower surface are higher than those tested from the upper surface, as the buried crack is closer to the lower surface than the upper surface. The above results show that the peak value of magnetic field intensity and gradient decreases with crack depth.

3.2 Impact of Applied Loads on MMM Signals

To study the impact of applied loads on the MMMS of a buried crack, welding specimen H1 was loaded as shown in Fig. 7.

The tensile load applied to the specimen was far lower than the yield strength, and no plastic deformation was observed in the crack tip according to the X-ray detection results.

Testing data of the magnetic field intensity and its gradient are shown in Figs. 8 and 9, which list the results at the lower surface of specimen H1 under an applied load of 15 kN.

A comparison of Figs. 8 and 9 reveals that under an applied load of 15 kN, there is an evident increase in the magnetic field intensity of the sample and its gradient. The maximum of the tangential component of the magnetic field intensity

Fig. 7 Test process of specimen H1 under applied load

reached 280 A/m and its gradient reached 35 (A/m)/mm, whereas the maximum of the normal component of the magnetic field intensity reached 400 A/m with a gradient of 130 (A/m)/mm. Therefore, inspecting cracks under working loads could yield better results than doing so under no
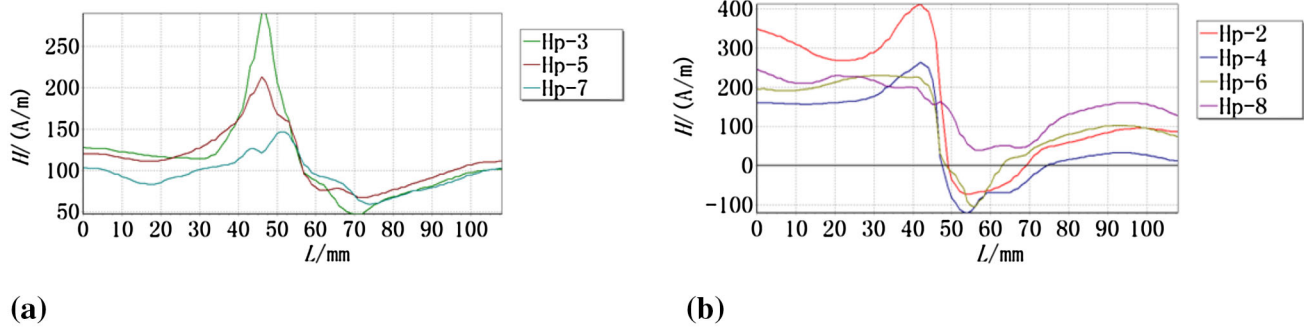
Fig. 8 Magnetic field intensity on the lower surface of specimen H1 under an applied load of 15 kN. **a** Tangential components. **b** Normal components
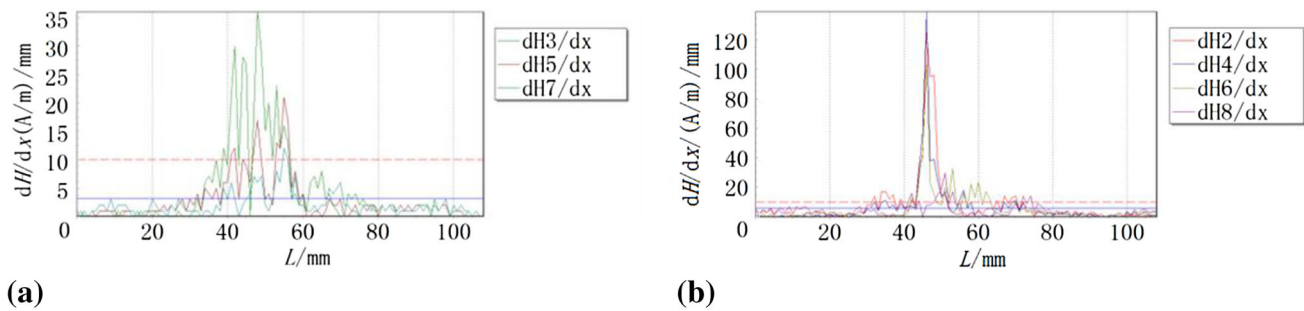

Fig. 9 Magnetic field gradient on the lower surface of specimen H1 under an applied load of 15 kN. **a** Gradient of tangential components. **b** Gradient of normal components
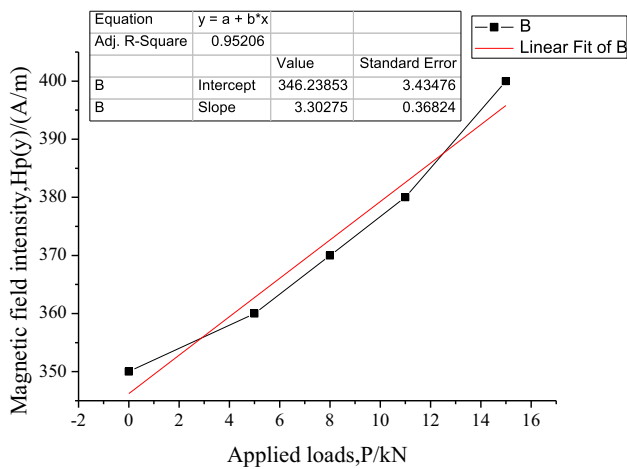

Fig. 10 Magnetic field intensity of specimen H2 as a function of applied load

Fig. 11 Process diagram of heat treatment

applied loads. MMM also appears to be suitable for detecting metal components subjected to applied loads.

For further analysis, the variation of the magnetic field intensity at the lower surface of the specimen with increasing applied loads is plotted in Fig. 10.

As can be seen in Fig. 9, the magnetic field intensity caused by the crack increased linearly with increasing load strength. This is because the applied loads lead to increased stress
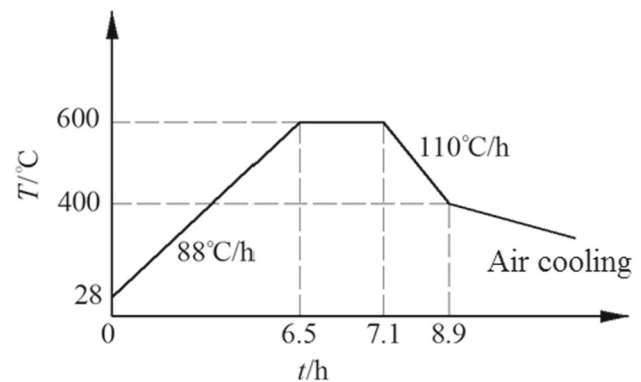
concentration in the specimen, and this stress can change the magnetization of ferromagnetic samples in term of piezo-magnetic effects. As a result, the magnetic field intensity increases with applied load [5].

3.3 Impact of Stress-Relieving Heat Treatment on MMM Signal

The SMFL of specimen H2 was recorded before heat treatment and compared with that of the specimen after heat treatment. The temperature profile of the stress-relieving heat treatment is shown in Fig. 11.
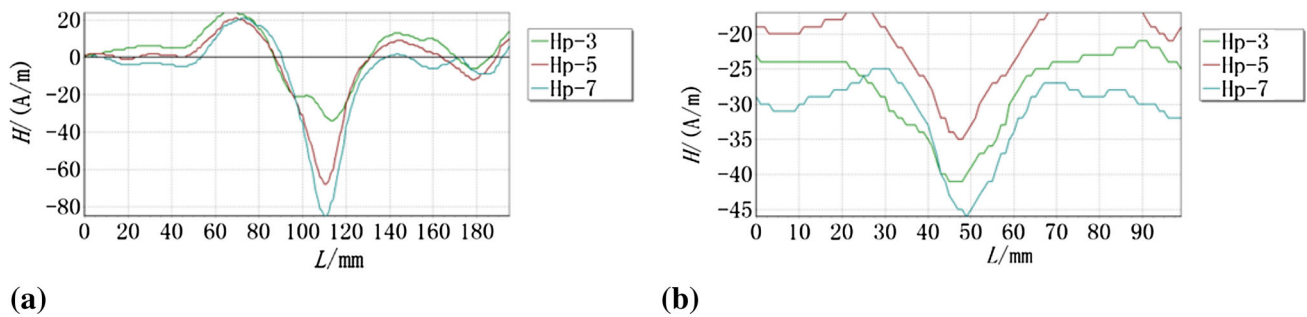
Fig. 12 Tangential components of magnetic field intensity. **a** Before heat treatment. **b** After heat treatment
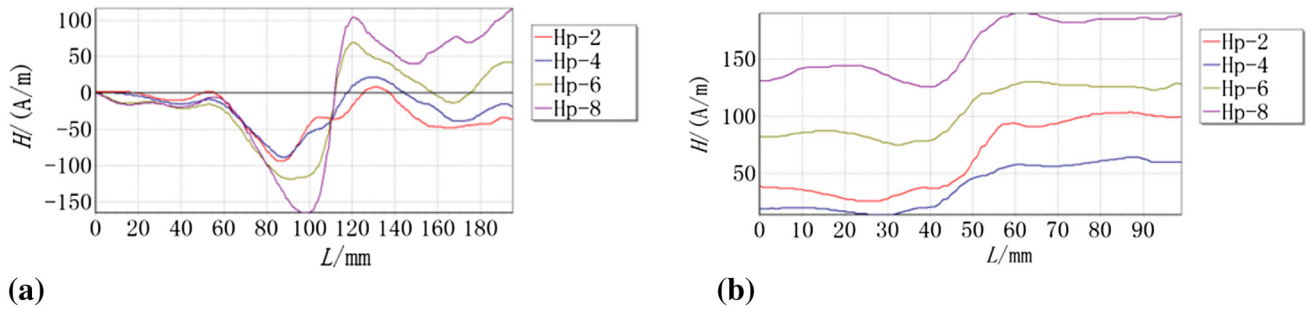

Fig. 13 Normal components of magnetic field intensity. **a** Before heat treatment. **b** After heat treatment
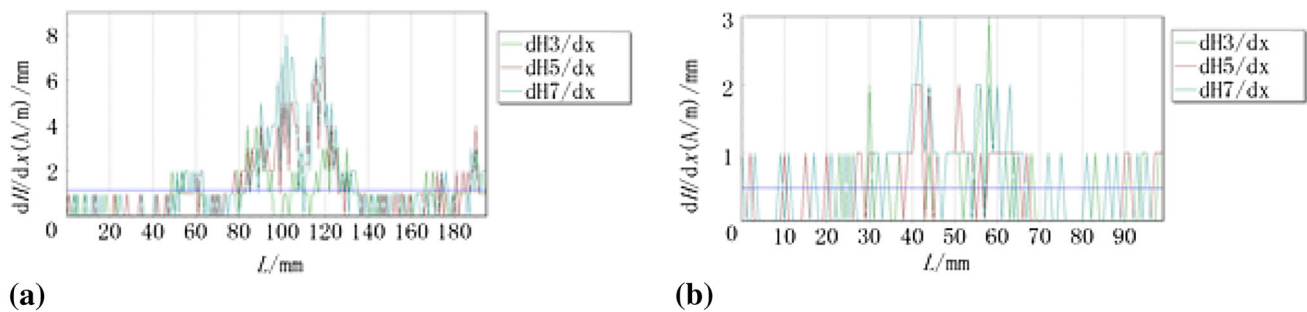

Fig. 14 Gradient of magnetic field intensity tangential components. **a** Before heat treatment. **b** After heat treatment
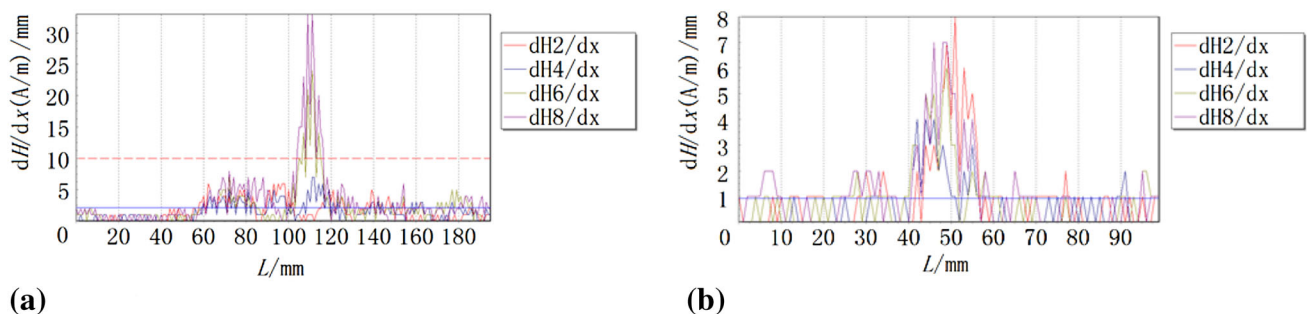

Fig. 15 Gradient of magnetic field intensity normal components. **a** Before heat treatment. **b** After heat treatment

Magnetic field intensity values before and after heat treatment are shown in Figs. 12 and 13.

As can be seen from Figs. 12 and 13, the maximum value of the tangential component of the magnetic field intensity is -80 A/m before heat treatment and −45 A/m after heat treatment, representing a 43.75% decrease. Similarly, the peak-valley value of the normal components of the magnetic field intensity is 250 A/m and 200 A/m before and after heat treatment, respectively, corresponding to a decrease of 20%.

Magnetic field intensity gradients before and after stress-relieving heat treatment of the cracked specimen are shown in Figs. 14 and 15.

As can be seen in Figs. 14 and 15, the change of magnetic field intensity gradient is quite apparent. Before heat treatment, the magnetic field intensity gradient of the odd and even channels reached 8 (A/m)/mm and 33 (A/m)/mm, respectively, whereas after heat treatment, these values were only 3 (A/m)/mm and 8 (A/m)/mm, reductions of 62.5 and 75.76%, respectively. One possible explanation for this is that the capacity of atomic activity increases with increasing temperature during heat treatment, and the movement of dislocations leads to decreased dislocation density, which continues until it completely disappears; this whole process is linked to decreased internal stress. In this process, the ordered domains caused by the original internal force disappear and return to a disordered state, decreasing the magnetic charge density and the magnetic field intensity.

4 Conclusions

Crack depth influences magnetic memory testing, in that the magnetic field intensity and its gradient decrease with increasing crack depth. The applied load of a sample also influences its MMMS. For the same crack, with an increase in applied load, the stress field caused by the crack increases and the magnetic field intensity and its gradient increase owing to magneto-mechanical effects. Therefore, MMM is suitable for inspecting metal components under working loads and with a high degree of accuracy. Finally, as an important process of metal machining, heat treatment can effectively eliminate the residual stress caused by welding or machining, but in terms of MMM testing, the influence of heat treatment on the magnetic memory signal must be considered. For the same crack defect, the magnetic memory test results are greatly attenuated by heat treatment, which significantly lowers the magnetic memory testing results compared to that observed before heat treatment.

References

1. Dubov, A.A.: Diagnostics of metal items and equipment by means of metal magnetic memory. In: Proceedings of the CHSNDT 7th Conference on NDT and International Research Symposium. Shantou China: Non-Destructive Testing Institution, CEMS:181–187 (1999)

2. Dubov, A.A.: Diagnostics of steam turbine disks using the metal magnetic memory method. Therm. Eng. **57**, 16–21 (2010)

3. Dubov, A.A.: Development of a metal magnetic memory method. Chem. Pet. Eng. **47**, 837–839 (2012)

4. Wang, Z.D., Gu, Y., Wang, Y.S.: A review of three magnetic NDT technologies. J. Magn. Mater. **324**, 382–388 (2012)

5. Wang, Z.D., Deng, B., Yao, K.: Physical model of plastic deformation on magnetization in ferromagnetic materials. J. Appl. Phys. **109**, 083928-1–083928-6 (2011)

6. Liu, B., Fu, Y., Jian, R.: Modeling and analysis of magnetic memory testing method based on the density functional theory. Nondestr. Test. Eval. **30**, 13–25 (2015)

7. Liu, B., Fu, Y., Xu, B.: Study on metal magnetic memory testing mechanism. Res. Nondestruc. Eval. **26**, 1–12 (2015)

8. Xu, M., Xu, M., Li, J., et al.: Metal magnetic memory field characterization at early fatigue damage based on modified Jiles-Atherton model. J. Cent. South Univ. **19**, 1488–1496 (2012)

9. Li, X., Ding, H., Bai, S.: Research on the stress-magnetism effect of ferromagnetic materials based on three-dimensional magnetic flux leakage testing. NDT&E Int. **62**, 50–54 (2014)

10. Leng, J., Liu, Y., Zhou, G., et al.: Metal magnetic memory signal response to plastic deformation of low carbon steel. NDT&E Int. **55**, 42–46 (2013)

11. Huang, H., Yao, J., Li, Z., et al.: Residual magnetic field induced by applied magnetic field and cyclic tensile stress. NDT&E Int. **63**, 38–42 (2014)

12. Huang, H., Jiang, S., Yang, C., et al.: Stress concentration impact on the magnetic memory signal of ferromagnetic structural steel. Nondestr. Test. Eval. **29**, 377–390 (2014)

13. Roskosz, M., Gawrilenko, P.: Analysis of changes in residual magnetic field in loaded notched samples. NDT&E Int. **41**, 570–576 (2008)

14. Roskosz, M.: Metal magnetic memory testing of welded joints of ferritic and austenitic steels [J]. NDT&E Int. **44**, 305–310 (2011)

15. Zhang, Y., Yang, S., Xu, X.: Application of metal magnetic memory test in failure analysis and safety evaluation of vessels. Front. Mech. Eng. China **4**, 40–48 (2009)

16. Leng, J., Xu, M., Xu, M., et al.: Magnetic field variation induced by cyclic bending stress. NDT&E Int. **42**, 410–414 (2009)

17. Roskosz, M., Bieniek, M.: Evaluation of residual stress in ferromagnetic steels based on residual magnetic field measurements. NDT&E Int. **45**, 55–62 (2012)

18. Yao, K., Shen, K., Wang, Z., et al.: Three-dimensional finite element analysis of residual magnetic field for ferromagnets under early damage. J. Magn. Mater. **354**, 112–118 (2014)

19. Dubov, A., Kolokolnikov, S.: The metal magnetic memory application for online monitoring of damage development in steel pipes and welded joint specimens. Weld. World **57**, 123–136 (2013)

20. Wang, Z.D., Yao, K., Deng, B., et al.: Theoretical studies of metal magnetic memory technique on magnetic flux leakage signals. NDT&E Int. **43**, 354–359 (2010)

21. Wang, Z.D., Yao, K., Deng, B., et al.: Quantitative study of metal memory signal versus local stress concentration. NDT&E Int. **43**, 513–518 (2010)